

Optically detected multipulse nuclear-quadrupole-resonance studies of trivalent praseodymium in zero and weak static magnetic fields

L. E. Erickson

National Research Council, Ottawa, Canada K1A 0R8

(Received 24 October 1988)

Optically detected multipulse nuclear quadrupole resonance is used to study trivalent praseodymium in lanthanum trifluoride in zero and weak static magnetic fields. A spin-locking spin-echo rf pulse sequence consisting of a $\pi/2$ preparation pulse, followed by repeated sequence of space t , a $\pi/2$ pulse phase shifted by 90° from the preparation pulse, and a space t . A Raman heterodyne scheme was used for optical detection. The coherence was observed to decay exponentially at a rate of $51 \mu\text{sec}$ (6.2 kHz) in zero static magnetic field. For static magnetic fields of 80 G applied along the c_3 axis the decay was described by time constants of $76 \mu\text{sec}$ (4.2 kHz) and $372 \mu\text{sec}$ (855 Hz). This represents a lengthening of the coherence time from a previously reported (two-pulse spin echo) $16.9 \mu\text{sec}$ (18.8 kHz) at zero field and a measured $37.5 \mu\text{sec}$ (8.5 kHz) at 80 G.

I. INTRODUCTION

Multipulse spin-echo techniques were first applied to pure nuclear quadrupole resonance by Marino and Klainer¹ as an attempt to improve the sensitivity of nuclear-quadrupole-resonance (NQR) spectroscopy in the same way that multipulse techniques had revolutionized high magnetic field NMR. The greatly enhanced NMR sensitivity (and resolution) obtained by this technique, which coherently averages some of the interactions that broaden the NMR lines, has provided a window into the study of many very weak interactions which were hidden in noise or masked by low resolution. Over the past ten years considerable effort has been expended in a number of laboratories on the study of van Vleck paramagnetic rare-earth ions in solids using both cw frequency and simple time domain techniques.²⁻¹⁰ These systems behave in many ways like pure nuclear quadrupole nuclei, with the exception that a large part of the "quadrupole" interaction is due to a second-order magnetic hyperfine interaction. This also produces an anisotropic magnetic tensor unlike that of pure quadrupole resonance. In this paper, the extension of multipulse techniques to van Vleck systems in zero or weak static magnetic fields using an optical detection technique is described.

II. THEORETICAL BACKGROUND

Subsequent to Marino and Klainer, the theory of multipulse NQR was described by Cantor and Waugh,¹¹ Zueva and Kessel,¹² and by Osokin¹³ with emphasis on the randomly oriented crystallites (powder) often used with NQR. More recently, Lee, Suter, and Pines¹⁴ have described a coherent averaging theory which generalizes the Hamiltonian to operators which are linear and bilinear in the spin coordinates and presents types of pulse sequences required to average specific Hamiltonian terms. All of these theories consider only isotropic magnetic tensors, and randomly oriented crystallites.

For Pr^{3+} in LaF_3 , the Hamiltonian may be written as a sum of three terms,

$$H = H_Q + H_D + H_F, \quad (1)$$

where

$$H_Q = D[I_z^2 - I(I+1)/3] + E(I_x^2 - I_y^2) \quad (2)$$

is the dominant term, and as the large static magnetic field in the NMR case, determines the quantization axis. $D=4.185$ MHz and $E=0.146$ MHz are interaction parameters which include both the second-order magnetic hyperfine (pseudoquadrupole) interaction and the pure quadrupole interactions from the lattice electric field gradient and that from the $4f$ electrons.

H_D is the dipolar Hamiltonian including both the Pr-Pr interactions and the Pr-F interactions. The former is very weak in this dilute situation.¹⁵

$$H_F = \sum_i (B_i \gamma_i) I_i \quad (3)$$

is the interaction in this weak magnetic field. Note that the enhanced magnetism is associated with the applied (static and rf pulsed) field, not with the nuclear spin.¹⁵ [In general, the axis system of the quadrupole moment differs from that of the anisotropic γ tensor. For this C_2 site symmetry, the γ axes are transformed into the quadrupole axes by a rotation around the symmetry-required y axis (C_2 axis) of 8.4° .¹⁶ This generates small off-diagonal terms in the γ tensor which can be ignored in this weak field.]

The details of the coherent averaging theory are beyond the scope of this paper. General treatises have been given by Haeberlen,¹⁷ Mehring,¹⁸ and Ernst *et al.*¹⁹ for NMR. For NQR, the paper of Lee *et al.*¹⁴ gives physical insight into the processes which lead to increased resolution (and sensitivity). Coherent averaging occurs because the resonant pulse sequence introduces a time dependence into some of the terms in the Hamiltonian which allows them to be averaged over time. Other terms have either no time dependence or a weak time dependence as a result of a particular pulse sequence. For example, the Carr-Purcell pulse sequence,

$$\pi/2 - (t - \pi - t)_n,$$

averages only terms linear in I_{jz} , such as the magnetic field inhomogeneity or the chemical shift. The more complex Waugh-Haeberlen-Huber four-pulse sequence,

$$\begin{aligned} &\pi/2(0)[-t - \pi/2(90) - 2t - \pi/2(-90) \\ &\quad - t - \pi/2(180) - t]_n, \end{aligned}$$

averages the $I_{jz}I_{kz}$ terms to zero and modifies (or scales) the chemical shift. (The number in parentheses indicates the relative phase of the rf pulse. The sequence in brackets is repeated.) In the NQR case, the chemical shift is zero and the static magnetic field inhomogeneity is negligible, but the unlike spin-spin terms, are large. The primary source of line broadening in $\text{LaF}_3:\text{Pr}^{3+}$ is Pr-F interactions. Haeberlen¹⁷ and Lee *et al.*¹⁴ point out that this behaves as a vector (not tensor) interaction, because only one spin species is stimulated by the rf pulse (e.g., heteronuclear interactions). The 80-G static magnetic field of some of these experiments is substantially greater than the local fields at the Pr nuclei. The consequence is a partially truncated Hamiltonian. Therefore, a simple pulse train should suffice in the weak static-field case, whereas a more complex pulse train would be required for substantial narrowing in the absence truncation at zero field. Lee *et al.*¹⁴ have suggested

$$[-\pi(0) - \pi(90) - \pi(0) - \pi(90)]_n,$$

as a possibility. Because $T_2 = 17 \mu\text{sec}$ in zero field, for $\text{LaF}_3:\text{Pr}^{3+}$, enormous amounts of rf power would be required in order to complete that cycle in times short compared to T_2 . This study, then, used the simpler spin-locking spin-echo pulse sequence,

$$\pi/2(90)[-t - \pi/2(0) - t]_n,$$

which was invented by Ostroff and Waugh.²⁰ The pulse sequences proposed by Lee *et al.*,¹⁴ which are tailored to eliminate or modify certain Hamiltonian terms, would permit selective study of the interactions present in the spin system.

III. EXPERIMENT

The experiment was similar to previous Raman heterodyne measurements²¹ in which magnetic resonance is detected by observing sidebands induced on a transmitted resonant light beam by a radio-frequency magnetic field interaction with the quadrupole moment (three-wave mixing). A $3 \times 3 \times 4\text{-mm}^3$ single-crystal $\text{LaF}_3:\text{Pr}^{3+}$, placed in a 6-mm-diam delay line coil²² with its C_3 axis parallel to the coil axis, was cooled to 2 K. The direction was chosen because all six Pr^{3+} sites are equivalent for magnetic fields in that direction.¹⁶ The crystal was irradiated by a focused (33 cm focal length) 10 mW cw light beam, parallel to the C_3 axis resonant with the $^1D_2\text{-}^3H_4$ transition (16873.06 cm^{-1}). A phase-stable rf pulse train was generated using a frequency synthesizer, a hybrid- T power splitter to obtain two rf phases separated by 90° , a fast quad rf switch, and a programmable transistor-transistor-logic (TTL) frequency counter to obtain rf pulses with an integral number of cycles. A data generator was used as a pulse programmer. A 50-W rf amplifier

was used to obtain peak fields of approximately 20 G. The rf pulse frequency was chosen to be at or near resonant with the $I_z = \frac{3}{2} - I_z = \frac{5}{2}$ transition in the ground level of the 3H_4 electronic state. As noted above, the spin-locking spin-echo pulse sequence²⁰ $\pi/2(90)[-t - \pi/2(0) - t]_n$ was used. The length of the $\pi/2$ pulse was determined by examining the nutation frequency during a long rf pulse. The optical sidebands were detected by an optical heterodyne receiver and were phase-sensitive demodulated using the same frequency synthesizer as a local oscillator. A Data Precision digital oscilloscope was used to average up to 1024 pulse trains at a repetition rate of 3 trains/sec. At higher repetition rates, the signal is reduced. The laser was frequency stabilized to a high-finesse (> 10000) Newport spherical Fabry-Perot interferometer using the rf-stabilization technique of Drever *et al.*²³ The laser linewidth is < 10 kHz for jitter frequencies $> 1\text{kHz}$, but the low-frequency jitter was about 100 kHz. The observed pulse trains were quite stable when viewed on an oscilloscope for sample temperatures of 5–6 K, but showed some amplitude variation at 2 K. This was attributed to the laser jitter being smaller than the phonon-induced optical linewidth of 1–3 MHz at the higher temperature, but not at the lower temperature where this width is much less than 1 kHz.²⁴ The rf magnetic field interacts with all of the Pr^{3+} ions, but the Raman heterodyne detector examines only those within the optical line.

A typical measurement, shown in Fig. 1, confirms that spin-locked spin echos are observed. The large pulse (off scale) at the beginning of the trace shows the free-induction decay (FID) due to the $\pi/2(90)$ preparation pulse. The next negative-going pulse structure is the FID due to the first $\pi/2(0)$ pulse. The positive-going pulse immediately following is the echo. Each $\pi/2(0)$ pulse is followed by a negative-going FID and a positive echo. If the phase of the rf reference is changed by 90° , the echo takes the shape of a dispersion curve. The echo pulses disappear if the $\pi/2(90)$ pulse is removed. This experimental result clearly demonstrates the connection between the preparation pulse and the spin echo, but the 38- μsec pulse separation, chosen here to clearly separate the FID from the echo, is larger than is desirable for multipulse spectroscopy. Note that the echo occurs at exactly halfway between pulses.

A zero-field multipulse measurement is shown in Fig. 2 with a cycle time $t_c = 2t + t_{\text{rf}} = 9.58 \mu\text{sec}$. The $\pi/2$ pulse length was $2.39 \mu\text{sec}$. This spectrum is the difference of two (1024 scans) measurements, one with a $\pi/2(90)$ preparation pulse and the other with no preparation pulse. This suppresses the FID signal and leaves the echo. The echo amplitude versus time is shown in Fig. 3. The data may be fitted to a simple exponential decay with lifetime $T_2^+ = 50.6 \pm 2.7 \mu\text{sec}$ (6.3 kHz). Shelby, Yannoni, and Macfarlane⁴ have reported $T_2 = 16.9 \mu\text{sec}$ (18.8 kHz) for a two-pulse echo.

From previous experiments it is known that T_2 is doubled when a weak static magnetic field, which is greater than the local superhyperfine fields, is applied.²¹ As a side benefit, the Raman heterodyne signals increase considerably in the presence of a field.²¹ Also, the small

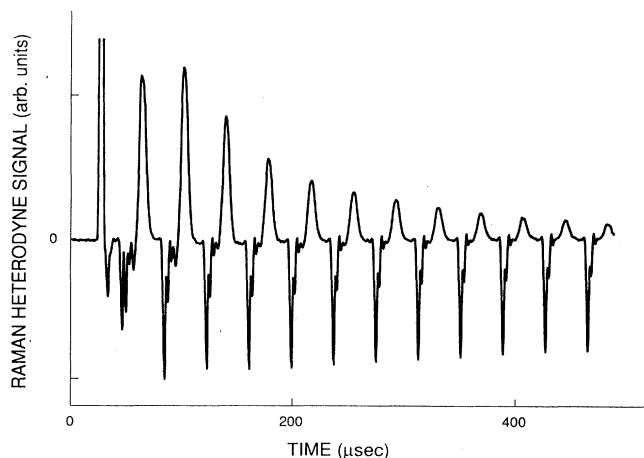


FIG. 1. A demonstration of spin-locking spin-echo NQR of Pr^{3+} in LaF_3 using a Raman heterodyne optical detection scheme. A static magnetic field of 80 G and a spin-locking spin-echo pulse sequence (rf magnetic field of 20 G), at 16.8 MHz (resonant with the $I_z = \frac{3}{2} - I_z = \frac{5}{2}$ transition), was applied to the same along the C_3 axis. A 10 mW frequency stabilized dye laser beam, resonant with the ${}^3H_4 - {}^1D_2$ optical transition (16873.08 cm^{-1}) illuminated the crystal along the C_3 axis. The data are the average of 256 scans. The rf pulse is at the leading edge of each structure, and is equal in width to width of the vertical line. The preparation pulse generates a positive FID. The negative-going structure is the free-induction decay following each repeated rf pulse. The echos are the large positive-going peaks halfway between the repeated rf pulses. The pulse cycle time is $38 \mu\text{sec}$ and the $\pi/2$ pulse length was $2.38 \mu\text{sec}$.

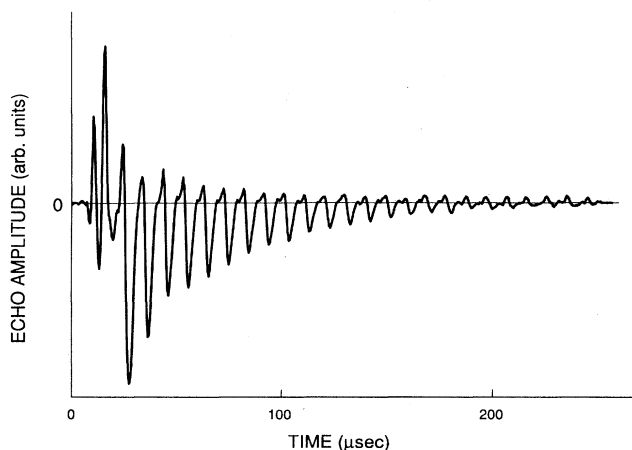


FIG. 2. A rf multipulse measurement of Pr^{3+} in single-crystal $\text{LaF}_3:\text{Pr}^{3+}$ at 2 K. The pulse train consists of equally spaced $\pi/2$ pulses. This curve is the difference between two (1024 scans) data sets, one with a single $\pi/2$ preparation pulse at one half the cycle time prior to the pulse train, whose rf is phase shifted by 90° from the pulse train, and a second with no preparation pulse. The radio frequency was 16.7 MHz. The cycle time is $9.58 \mu\text{sec}$ and the $\pi/2$ pulse length is $2.39 \mu\text{sec}$.

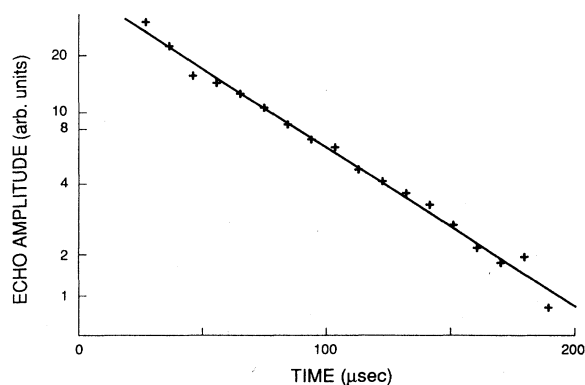


FIG. 3. A plot of the Fig. 2 echo peak amplitudes vs time is shown together with a linear regression fit to the data. The decay time for this data is $50.6 \pm 2.7 \mu\text{sec}$.

magnetic field will partially truncate the Hamiltonian. The longer lifetime and the partially truncated Hamiltonian should lead to a longer decay time T_2^+ . The quantization axis continues to be determined by the dominant quadrupole interaction in this weak-field regime. A multipulse measurement of $\text{LaF}_3:\text{Pr}^{3+}$ in a static magnetic field of 80 G along C_3 is shown in Fig. 4. The static and rf magnetic fields and the light beam are colinear. The rf frequency is now 16.9 MHz which is near but not resonant with the 16810 kHz, $I_z = +\frac{5}{2} - I_z = +\frac{3}{2}$ transition, and is separated from the $I_z = -\frac{5}{2} - I_z = -\frac{3}{2}$ transition at 16550 kHz. The rf pulse duration $t_{\text{rf}} = 2.01 \mu\text{sec}$ (34 cycles) and the cycle time $t_c = 16.09 \mu\text{sec}$. Because of the reduced inhomogeneous width, a longer cycle time was required to avoid the free-induction decay signal.

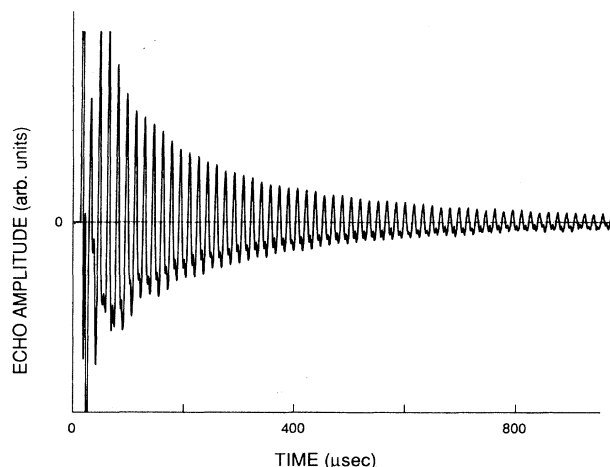


FIG. 4. The rf multipulse measurement of Pr^{3+} in single-crystal $\text{LaF}_3:\text{Pr}^{3+}$ at 2 K in a static magnetic field of 80 G directed along the C_3 axis of the crystal. The cycle time is 16.09 sec and the $\pi/2$ pulse length is $2.01 \mu\text{sec}$. The radio frequency was 16.9 MHz. The pulse sequence is described in Fig. 1 and in the text. These data are a difference between two 1024 scan averages, with and without the preparation pulse.

One observes a greatly increased decay time which is described by two exponential decays with time constants T_2^+ equal to $76 \pm 13 \mu\text{sec}$ (4.2 kHz) and $372 \pm 45 \mu\text{sec}$ (0.86 kHz), as shown in Fig. 5. This should be compared to our Raman heterodyne ($\pi/2-t-\pi-t$ -echo) measurement of $T_2 = 37.5 \pm 1.3 \mu\text{sec}$ (8.5 kHz) under identical conditions. Wong *et al.*²¹ reported $29 \mu\text{sec}$ (11 kHz) in a magnetic field of 30 G.

IV. DISCUSSION

The lengthened decay times T_2^+ observed, originate from averaging of the heteronuclear dipolar Hamiltonian which is responsible for the observed T_2 . The fact that they are not even longer is due to NMR-NQR coherence sustaining concerns such as the cycle time not being short compared to T_2 , because of pulse errors, e.g., rf field inhomogeneity, timing errors, and length not exactly $\pi/2$, and to Raman heterodyne detection concerns such as optical pumping during the pulse train. In multipulse experiments, the decay time T_2^+ has been shown to have a t^{-2} to t^{-5} dependence on the cycle time:^{25,26} e.g., a t^{-5} dependence was measured by Marino and Klainer¹ in their NQR study. It is important that the cycle time is less than the dephasing time T_2 . The cycle time is usually limited by the available rf power (pulsewidth) and by the rf inhomogeneous linewidth of the material, both of which govern the length of the free-induction decay after each pulse. For the zero-field experiment, a cycle time of $10 \mu\text{sec}$ was long enough to prevent the FID from hiding the echo. The limited available rf power required pulses of approximately $2 \mu\text{sec}$. In the 80G weak-field measurements, the FID is longer, so a $16\text{-}\mu\text{sec}$ or longer cycle

time was appropriate. The excitation volume in the sample is a small-diameter cylinder parallel to and near the axis of the coil. This should minimize the radial rf field inhomogeneities. Axial inhomogeneities are a more serious problem. Attempts to probe the field along the axis were inconclusive. The pulse timing is phase locked to the rf frequency and is precisely controlled. The largest pulse error is in the determination of the exact $\pi/2$ rf pulse length. This is done by a measurement of the nutation frequency at the same rf magnetic field. Ostroff and Waugh,²⁰ however, have pointed out that the long-time dependence does not critically depend on the pulse length being $\pi/2$. The T_2^+ dependence on cycle time was measured for fields of 80 G and for cycle times of up to $75 \mu\text{sec}$. The results did *not* demonstrate a strong lifetime dependence but did show a strong amplitude effect. At the longer cycle times, the signals were too weak, so only a few echos are observed which preclude an accurate measurement.

The optical pumping produces a substantial nuclear polarization which is responsible for the big signal. Since the light level required for Raman heterodyne detection is greater than that required to produce this nuclear polarization, and the light beam is not attenuated during the pulse sequence, it is reasonable to ask what is the effect of optical pumping on the decay time. A pumped coherent spin is removed from the observed level for an optical lifetime (0.5 ms) which would reduce the echo signal. During that time, it would experience pulse angles that are different than for the ground state, because the excited state γ differs considerably from that of the ground state. Consequently, when it returns to its origi-

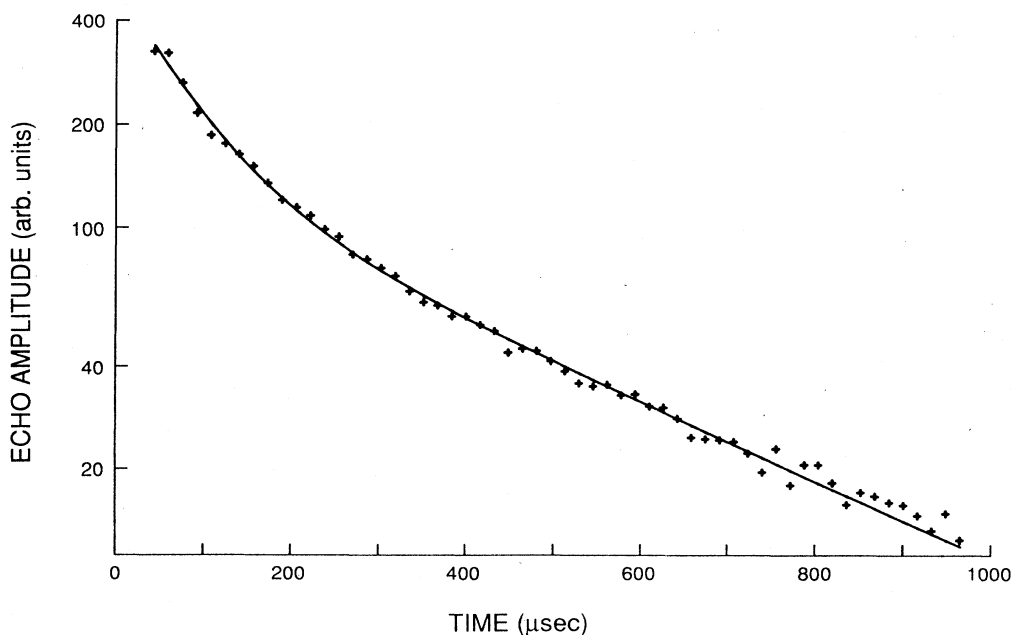


FIG. 5. A plot of the Fig. 4 peak echo amplitudes vs time is shown together with a nonlinear regression fit of sum of two exponential functions. The decay times are 76 ± 13 and $372 \pm 45 \mu\text{sec}$.

nal state, it will not contribute coherently to the signal. Some of the pumped ions will not return to the original state because the asymmetry of the quadrupole interaction results in optical branching to other ground-state hyperfine levels, where they remain for seconds. Nor would those that are introduced after the preparation pulse contribute to the coherent signal. The length of time an average ion remains undisturbed by the light may be estimated, knowing the light level and bandwidth, the optical absorption and the Pr^{3+} concentration and other experimental parameters. The beam waist is 0.12 mm in diameter and 3.6 cm long, so a cylindrical volume of $4.5 \times 10^{-5} \text{ cm}^3$ of the crystal is excited. This cylindrical volume contains 2.9×10^{16} Pr^{3+} ions over an optical spectral range of approximately 4 GHz. If we assume a laser bandwidth of 1 MHz, then about 6.5×10^{12} ions participate. A 10-mW laser beam has a flux of 3×10^{16} photons/sec. Now the unsaturated optical absorption is about 5%, but under the steady-state conditions of this experiment the absorption is estimated to be about 100 times less, or an average ion interacts with a laser photon every 20 ms. This indicates that the optical pumping should not be a major factor in determining the multipulse lifetime of these experiments, but will be a limiting lifetime of this Raman heterodyne technique. Its effect may be reduced by gating the light during the rf pulse train, and sampling the coherence optically for brief periods. The optical pumping effects were measured by gating the light off with an electro-optic modulator (100:1 contrast) just prior to the $\pi/2$ preparation pulse, and turning it on just before the n th echo. The amplitude of the (unpumped) n th echo was then compared to that for a nongated experiment. To first order, the decay appeared similar to the nongated experiment. The n th pulse was some 20–30% larger in amplitude than the same echo not gated. With the optical pumping resumed, the pulse trains were exactly the same amplitude after 250 μsec . The lifetime was checked by examining cycle (unpumped) echoes at 85- μsec intervals (28.5 μsec cycle time, 80 G along C_3 , 16.8 MHz), with a simple exponential regression fit, and was found to be about 20% longer than for the ungated run made under the same conditions. This was a crude comparison. An accurate comparison will require a more sophisticated gating control than was used. Obviously, optical pumping must be considered. It is a significant but not a dominant contributor to the lifetime in these experiments.

The decay time in multipulse NMR experiments depends also upon the spin-lattice relaxation. This has been discussed by Haeberlen and Waugh²⁷ using a perturbation model where both the spin-lattice relaxation and the externally produced periodic disturbances are included. They estimate the relaxation effect on spin-locking experiments using a Gaussian-Markoff model of spin-lattice relaxation in an effective field B_{rf} in the rotating frame,

$$1/T_{1p} = M_2 \tau_c / (1 + 4\omega_e^2 \tau_c^2), \quad (4)$$

where τ_c is the Gauss-Markoff correlation time, $\omega_e = \gamma_x B_{\text{rf}}$ and M_2 is the second moment which is nearly

equal to T_2^{-2} . Mehring²⁸ has shown that the maximum relaxation effects occurs for $\omega_e \tau_c = \frac{1}{2}$ and is

$$T_1/T_2 = 4\gamma_x B_{\text{rf}}/M_2^{1/2}. \quad (5)$$

Applying Eq. (5) to the NQR situation, one would expect a limiting decay time as short as $100T_2$. ($B_{\text{rf}} = 20$ G, $M_2^{1/2} = 4$ G and $\gamma_x = 5$ kHz/G were assumed.)

Other NMR line-narrowing techniques have been used on $\text{LaF}_3:\text{Pr}^{3+}$ to narrow the optical transition between the ground 3H_4 state and the lowest 1D_2 state. The dominant source of the homogeneous line-broadening mechanism is the same for both the 3H_4 (0 cm^{-1})– 1D_2 (16873 cm^{-1}) optical transitions and the ground-state 3H_4 (0 cm^{-1}) NQR transition of this work. That source is the fluctuating magnetic fields at the Pr nucleus due to neighboring F nuclei spin flips. The work of Rand *et al.*⁹ used a well-known NMR technique of detuned rf irradiation of the F nuclear spins to cause them to precess at the magic angle around the static magnetic field. This analog of magic angle spinning introduces a periodicity into the Hamiltonian to average the dipolar interaction between the F nuclei and the Pr nuclei. Using optical free-induction decay and they found optical linewidths narrowed from 10 to 3 kHz. Macfarlane *et al.*¹⁰ used the same method with higher static and rf magnetic fields, both on resonance (and off resonance) during a photon-echo sequence, and they observed optical line narrowing from 56 kHz without decoupling to 6 kHz (4 kHz) with decoupling. In general, the optical linewidths will be different than the NQR widths because the enhanced nuclear magnetism differs considerably from state to state, and because the optical transitions include all nuclear substates.

V. CONCLUSION

Multipulse NQR of the van Vleck paramagnetic ion Pr^{3+} , has been demonstrated in zero and low static magnetic fields using a Raman heterodyne optical detection technique, which avoids the field cycling schemes needed with conventional NMR detection. The spin-locking spin-echo sequence used produced a lengthening of the coherence decay time from 37 to 372 μsec in static fields of 80 G. In the absence of a static magnetic field, the effect was less dramatic, from 17 to 51 μsec . This is likely due to the more complex Hamiltonian because all of the local fields are involved, unlike the low-field case where the static field is greater than the local fields. Optical pumping was shown to contribute to a small but significant reduction of the coherence time. These longer lifetimes demonstrates the quality of the experiment and are not a measure of some internal process such as the spin-lattice relaxation in the rotating frame. They do however, open a window to measure internal interactions because of the extended coherence time. Experimental improvements, such as rf coil design, more rf power, and more complex pulse sequences, should lead to even longer lifetimes and the possibility of examining multiquantum NQR.

- ¹R. A. Marino and S. M. Klainer, *J. Chem. Phys.* **67**, 3388 (1977).
- ²M. A. Teplov, *Zh. Eksp. Teor. Fiz.* **53**, 1510 (1967) [*Sov. Phys.—JETP* **26**, 872 (1968)].
- ³L. E. Erickson, *Opt. Commun.* **21**, 147 (1977).
- ⁴R. M. Shelby, C. S. Yannoni, and R. Macfarlane, *Phys. Rev. Lett.* **41**, 1739 (1978).
- ⁵K. Chiang, E. A. Whittaker, and S. R. Hartmann, *Phys. Rev. B* **23**, 6142 (1981).
- ⁶B. Bleaney, F. N. H. Robinson, and M. R. Wells, *Proc. R. Soc. London, Ser. A* **362**, 179 (1978).
- ⁷J. Mlynek, N. C. Wong, R. G. DeVoe, E. S. Kintzer, and R. G. Brewer, *Phys. Rev. Lett.* **50**, 993 (1983).
- ⁸A. J. Silversmith, and N. B. Manson, *J. Phys. C* **17**, L97 (1984).
- ⁹S. C. Rand, A. Wokaun, R. G. DeVoe, and R. G. Brewer, *Phys. Rev. Lett.* **43**, 1868 (1979).
- ¹⁰R. M. Macfarlane, C. S. Yannoni, and R. M. Shelby, *Opt. Commun.* **32**, 101 (1980).
- ¹¹R. S. Cantor and J. S. Waugh, *J. Chem. Phys.* **73**, 1054 (1980).
- ¹²O. S. Zueva and A. R. Kessel, *Fiz. Tverd. Tela (Leningrad)* **21**, 3518 (1979) [*Sov. Phys.—Solid State* **21**, 2032 (1979)].
- ¹³D. Ya. Osokin, *Phys. Status Solidi B* **102**, 681 (1980).
- ¹⁴C. J. Lee, D. Suter, and A. Pines, *J. Magn. Res.* **75**, 110 (1987).
- ¹⁵A. Abragam and B. Bleaney, *Proc. R. Soc. London, Ser. A* **387**, 221 (1983).
- ¹⁶B. R. Reddy and L. E. Erickson, *Phys. Rev. B* **27**, 5217 (1983).
- ¹⁷U. Haeberlen, in *High Resolution NMR in Solids*, Suppl. 1 of *Advances in Magnetic Resonance*, edited by John Waugh (Academic, New York, 1976).
- ¹⁸M. Mehring, in *Principles of High Resolution NMR in Solids*, Vol. II of *NMR Basic Principles and Progress*, edited by P. Diehl, E. Fluck, and R. Kosfeld (Springer-Verlag, Berlin, 1983), 2nd ed.
- ¹⁹R. R. Ernst, G. Bodenhausen, and A. Wokaun, *Principles of Magnetic Resonance in One and Two Dimensions* (Clarendon, Oxford, 1987).
- ²⁰E. D. Ostroff and J. S. Waugh, *Phys. Rev. Lett.* **16**, 1097 (1966); P. Mansfield and D. Ware, *Phys. Lett.* **22**, 133 (1966).
- ²¹N. C. Wong, E. S. Kintzer, J. Mlynek, R. G. DeVoe, and R. G. Brewer, *Phys. Rev. B* **28**, 4993 (1983).
- ²²I. J. Lowe and M. Engelsberg, *Rev. Sci. Instrum.* **45**, 631 (1974).
- ²³R. W. P. Drever, J. L. Hall, F. V. Kowalski, J. Hough, G. M. Ford, A. J. Munley, and H. Ward, *Appl. Phys. B* **31**, 97 (1983).
- ²⁴L. E. Erickson, *Opt. Commun.* **15**, 246 (1975).
- ²⁵W. K. Rhim, D. D. Elleman, and R. W. Vaughan, *J. Chem. Phys.* **59**, 3740 (1973).
- ²⁶M. Mehring, in Ref. 18, Sec. 3.8.
- ²⁷U. Haeberlen and J. S. Waugh, *Phys. Rev.* **185**, 420 (1969).
- ²⁸M. Mehring, in Ref. 18, Sec. 8.2.